

Jean-François Oudkerk
e-mail: jfoudkerk@ulg.ac.be

Sylvain Quoilin

Sébastien Declaye

Ludovic Guillaume

Thermodynamics Laboratory,
University of Liège,
Campus du Sart-Tilman, B-49,
B-4000 Liège, Belgium

Eric Winandy

Emerson Climate Technologies GmbH,
Pascalstrasse 65,
52076 Aachen Germany

Vincent Lemort

Thermodynamics Laboratory,
University of Liège,
Campus du Sart-Tilman, B-49,
B-4000 Liège, Belgium

Evaluation of the Energy Performance of an Organic Rankine Cycle-Based Micro Combined Heat and Power System Involving a Hermetic Scroll Expander

This paper evaluates the performance of an organic Rankine cycle (ORC) based micro-combined heat and power (CHP) unit using a scroll expander. The considered system consists of a fuel boiler coupled with an ORC engine. As a preliminary step, the results of an experimental campaign and the modeling of a hermetic, lubricated scroll compressor used as an expander are presented. Then, a fluid comparison based on several criteria is conducted, leading to the selection of R245fa as working fluid for the ORC. A simulation model is then built to evaluate the performance of the system. The model associates an ORC model and a boiler model, both experimentally validated. This model is used to optimize and size the system. The optimization is performed considering two degrees of freedom: the evaporating temperature and the heat transfer fluid (HTF) mass flow rate. Seasonal simulation is finally performed with a bin method according to the standard PrEN14825 for an average European climate and for four heat emitter heating curves. Simulation results show that the electrical efficiency of the system varies from 6.35% for hot water at 65 °C (high temperature application) to 8.6% for a hot water temperature of 22 °C (low temperature application). Over one entire year, the system exhibits an overall electrical efficiency of about 8% and an overall thermal efficiency around 87% without significant difference between the four heat emitter heating curves. Finally, some improvements of the scroll expander are evaluated. It is shown that by increasing the maximum inlet temperature (limited to 140 °C due to technical reasons) and using two scroll expanders in series, the overall electrical efficiency reaches 12.5%.

[DOI: 10.1115/1.4023116]

1 Introduction

Combined heat and power (CHP) refers to the production of electrical (or mechanical) power and useful heat simultaneously. This way to produce heat and electricity leads to a reduction of primary energy consumption and, in most cases, a reduction of greenhouse gas emissions. Therefore, in the current energy and environmental context (depletion of fossil fuels and climate change), the interest in CHP is growing. Special attention is currently paid to small-scale CHP such as micro-CHP (<50 kWe) because it is not widely implemented while it offers an alternative to large-scale CHP [1–5]. Moreover, CHP is within the scope of decentralized energy production, one of the key issues in the energy sectors of the European Union.

The main technologies available for micro-CHP at the present time are the internal combustion engine (ICE), the Stirling engine, and fuel cells that are already marketed and the microgas turbine and the ORC that are still in development [6]. Table 1 summarizes the main characteristics of each technology (in this table, electrical efficiency is the ratio between electrical power output and fuel power input; total efficiency is the sum of electrical efficiency and thermal efficiency, which is the ratio between heat power output and fuel power input). The technologies giving the best efficiencies are ICE and fuel cell but have the drawback of internal combustion

and, thus, are limited in fuels. Fuel cell systems still show very high costs and have a very limited lifetime. Microturbines are not suitable for micro CHP because of their poor electrical efficiency at low scale and the high temperature of heat generated is more suitable for industrial process than for building heating. Finally, the two external combustion engines, namely the ORC and the Stirling engines, are comparable in terms of electrical efficiency. However, they show the advantage of fuel flexibility that can lead to use of renewable fuels such as biomass or solar energy.

Scroll machines are particularly well adapted to small-scale Rankine cycle applications (electrical outputs lower than 25 kWe) and offer major advantages such as reliability and robustness (reduced number of moving parts), simplicity (no admission and discharge valves), low rotational speeds and ability to handle high pressure ratios [7]. Numerous scientific studies on ORC systems using scroll expanders are available and show the technical interest for this kind of engine [7–11].

This paper aims at evaluating the performance of an ORC-based micro-CHP unit using a hermetic scroll compressor turned into expander mode. The system consists of a fuel boiler coupled with an ORC. The first part of the paper presents the results of an experimental campaign and the modeling of a hermetic, lubricated scroll compressor used as an expander. Then, two fluid selection criteria related to the cycle performance and to the constraints of hermetic scroll expanders are proposed and different fluids are compared to select the best one. A simulation model is built by assembling different submodels of each component: fuel oil boiler, heat exchangers, scroll expander, and working fluid pump.

Contributed by the International Gas Turbine Institute (IGTI) of ASME for publication in the JOURNAL OF ENGINEERING FOR GAS TURBINES AND POWER. Manuscript received February 29, 2012; final manuscript received October 11, 2012; published online March 18, 2013. Assoc. Editor: Paolo Chiesa.

Table 1 Comparison of the different technologies of m-CHP

	ICE	Microturbine	Stirling	ORC	Fuel cell
Electrical power	5 kWe–20 MWe	15 kWe–300 kWe	1 kWe–1.5 MWe	1 kWe–10 MWe	1 kWe–1 MWe
Electrical efficiency	25–45%	15–30%	10–20%	~10%	30–70%
Total efficiency	65–92%	65–90%	65–95%	~90%	90%
Fuel	Gasoline, diesel, gas, biogas,...	Gas, biogas,...	Flexible	Flexible	Hydrogen or hydrogen-rich gas
State	Widespread	Uncommon	Development, early market	Development, early market	Proven technology

This model is used to size the system (heat exchanger area and expander’s swept volume), using an optimization algorithm and exploiting the two available degrees of freedom, i.e., evaporating temperature and heat transfer fluid (HTF) mass flow rate. Off-design performance is then evaluated and seasonal simulations are run on a yearly basis. Guidelines for the improvement of the scroll expander are finally provided with a view to maximizing the performance of such a system.

2 Experimental Investigation of a Hermetic Scroll Expander

This section summarizes the main experimental results obtained with a hermetic scroll compressor modified to work in expander mode. The compressor tested is a Copeland compressor type ZH30K4E-TFD and the working fluid is R245fa. An exhaustive description of the test bench was proposed previously by some of the authors [7].

In order to evaluate the performance of the expander, two indicators are used:

The overall isentropic effectiveness:

$$\epsilon_s = \frac{\dot{W}}{\dot{M} \cdot (h_{su} - h_{ex,s})} \tag{1}$$

The filling factor:

$$FF = \frac{\dot{M} \cdot v_{su}}{\dot{V}_s} \tag{2}$$

It should be noted that the definition of the isentropic effectiveness based on a ratio of specific enthalpy difference cannot be used in this case because this definition is valid for adiabatic processes only. In the case of volumetric expanders, even insulated devices exchange a nonnegligible amount of heat with their environment. The relation between both definitions can be obtained by combining Eq. (1) with the first law of thermodynamics:

$$\begin{aligned} \epsilon_s &= \frac{\dot{W}}{\dot{M} \cdot (h_{su} - h_{ex,s})} = \frac{\dot{M} \cdot (h_{su} - h_{ex}) - \dot{Q}_{amb}}{\dot{M} \cdot (h_{su} - h_{ex,s})} \\ &= \frac{h_{su} - h_{ex}}{h_{su} - h_{ex,s}} - \frac{\dot{Q}_{amb}}{\dot{M} \cdot (h_{su} - h_{ex,s})} \end{aligned} \tag{3}$$

Equation (3) shows that both definitions only agree if the ambient heat losses \dot{Q}_{amb} are negligible.

The measured isentropic effectiveness is plotted for each test as a function of the pressure ratio in Fig. 1. This isentropic effectiveness sharply decreases for low pressure ratios because of overexpansion losses and decreases at larger pressure ratios because of underexpansion losses [9]. The achieved maximum overall isentropic effectiveness is 73%.

Lemort et al. [7] adapted a semiempirical model previously proposed for an open-drive scroll expander [8] to describe the behavior of the hermetic expander under various working conditions. The proposed model accounts for the main physical features of the machine and for different sources of losses such as internal

leakage, friction, pressure drop, heat transfers, and under- and overexpansion losses. The model input variables are the supply and exhaust pressures and the supply temperature. The output variables are the mass flow rate displaced by the expander, its electrical power production, and the exhaust working fluid temperature. It was shown that the maximal deviation between model predictions and experimental data is 2.5% for the mass flow rate and 5% for the shaft power. This model will be used in this work in order to evaluate some possible improvements of the expander.

The identified parameters of the above model are valid for a specific machine only. Polynomial curves of the effectiveness are better adapted to system simulation (simulate the expander in the micro-CHP system) because they are nondimensional and can be applied to various expander sizes. However, they require a relatively high number of parameters that cannot be determined on the basis of the available experimental data points. Therefore, the semiempirical model is used to express ϵ_s and FF as polynomial laws of the main working conditions. The two selected working conditions are the inlet pressure P_{su} and the pressure ratio over the expander r_p . The polynomial fits are expressed in the following form:

$$\epsilon_s = \sum_{i=0}^{n-1} \sum_{j=0}^{n-1} a_{ij} \cdot (\ln(r_p))^i \cdot (\ln(P_{su}))^j = f(r_p, P_{su}) \tag{4}$$

For ϵ_s , a fourth-order ($n=4$) polynomial fit is used, while for FF a second-order ($n=2$) polynomial fit turned out to be sufficient. The correlations have been established on the basis of the validated model within the following ranges of operating conditions:

$$2.10^5 < P_{su} < 35.10^5 \text{ Pa}; \quad 1.7 < r_p < 20$$

The values of ϵ_s and FF were, respectively, predicted by the polynomial fits with $R^2 = 99.31\%$ and $R^2 = 99.62\%$.

It is assumed that, when changing the scale of the expander (and, thus, the swept volume), the isentropic effectiveness and the filling factor remain similar if the pressure ratio and the inlet

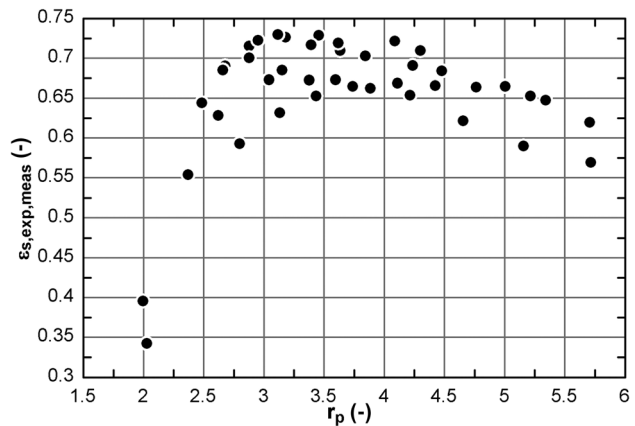


Fig. 1 Evolution of the overall isentropic effectiveness with the pressure ratio imposed to the expander

density are kept equal. These two performance indicators are the ones that are selected for the further developments presented in this paper.

3 Losses and Selection Criteria

Several sources of losses affect the isentropic effectiveness of the expander. These sources are [7]:

- supply pressure drop: during the suction process
- heat transfers: during suction and exhaust (the expansion is considered adiabatic)
- mechanical losses: due to the friction
- internal leakage: due to the gap between moving elements
- over- or underexpansion: due to the fixed built-in volume ratio
- electromechanical losses: due to the losses in the generator

Among these different sources of losses, two are related to ORC operating conditions: over- or underexpansion losses and electromechanical losses.

Indeed, under or over expansion losses depend on the internal built-in volume ratio $r_{v,in}$, characteristic of the expander, while the external volume ratio $r_v = v_{su,exp}/v_{ex,exp}$ is imposed by the working conditions (fluid and level of temperatures/pressures). Under- and overexpansion losses disappear when the internal built-in volume ratio is equal to the external volume ratio $r_{v,in} = r_v$.

In this work, electromechanical losses refer to the electrical generator losses. They are mainly a function of the shaft power, as shown in Fig. 2 for a typical scroll engine: The efficiency of the generator ($\eta_{generator} = \dot{W}_{el}/\dot{W}_{sh}$) is above 84% for a shaft power between $\dot{W}_{sh,max}/4$ and $\dot{W}_{sh,max}$ (the maximal shaft power of the generator). In a volumetric hermetic device, this range of power depends on the displacement, indeed the bigger the displacement the larger the power. Then a hermetic device can be characterized by the ratio between the displacement and the power of the generator (see Eq. (5)); in this work, this ratio will be called the volume coefficient (CV). Figure 2 shows this volume coefficient for a typical scroll compressor in term of shaft power and it appears that it is included between 0.19 and 0.82 m^3/MJ to have a generator efficiency upper than 84%. In an ORC, the power is expressed by Eq. (6) and by combining with Eq. (5), the volume coefficient of the ORC is found (see Eq. (7)). The volume coefficient of the ORC depends only on the working fluid and on the level of pressure. In order to have a good generator efficiency, the CV_{ORC} needs to match with the CV_{exp} . If it is smaller than the lower limit (0.19 m^3/MJ in this case), it means that the generator is undersized and, conversely, if it is bigger than the upper limit (0.82 m^3/MJ), it means that the generator is oversized. The volume coefficient of the ORC is also an indicator of the compactness of all the system.

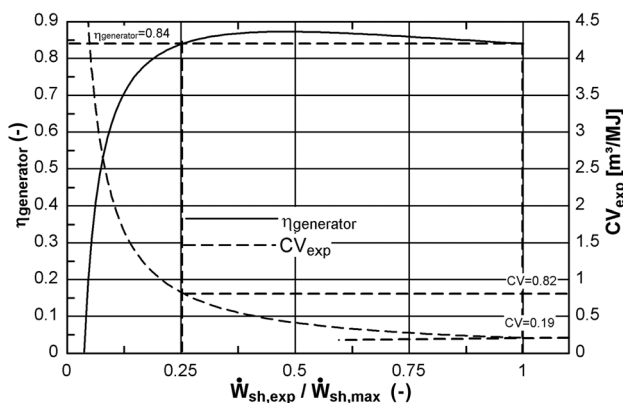


Fig. 2 Efficiency of the generator and CV_{exp} versus shaft power for a typical scroll expander

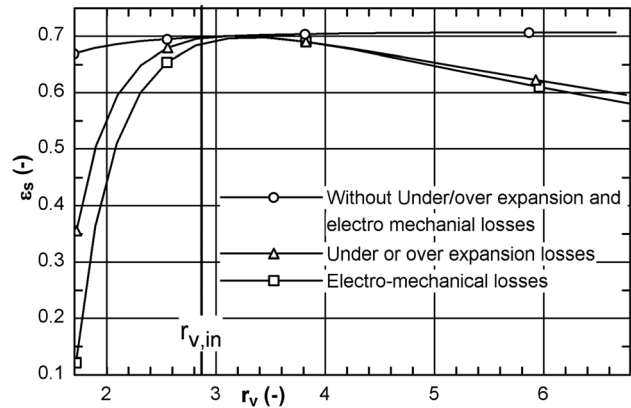


Fig. 3 Contribution of electromechanical and under- or over-expansion losses

Indeed, for a given power, the larger the CV, the larger the volume of the main components (evaporator and condenser).

$$CV_{exp} = \frac{\dot{V}_{exp}}{\dot{W}_{sh,exp}} = \frac{\dot{V}_{exp}}{\dot{W}_{el,exp}} \cdot \eta_{generator} \quad (5)$$

$$\dot{W}_{sh,max} = \dot{M}_{exp} \cdot \Delta h_{exp} = \frac{\dot{V}_{exp}}{v_{su,exp}} \cdot \Delta h_{exp} \quad (6)$$

$$CV_{ORC} = \frac{v_{su,exp}}{\Delta h_{exp}} \quad (7)$$

Figure 3 shows the evolution of the isentropic effectiveness with the volume ratio imposed to the expander for R245fa. The black line shows the efficiency if the internal volume ratio was always adapted to the external volume ratio and if the generator efficiency was always maximal. The blue line shows the evolution of the isentropic effectiveness with under- and overexpansion losses and finally, the red line shows the evolution with all sources of losses. The small difference between the internal volume ratio ($r_{v,in} = 2.85$) and the external volume ratio that maximizes the isentropic effectiveness is due to the supply pressure drop.

4 Design of the Micro-CHP System

The selected configuration of the ORC-based CHP unit is shown in Fig. 4: The fuel oil boiler heats up a heat transfer fluid (HTF); this HTF passes through the evaporator of the ORC where it preheats, evaporates, and eventually superheats the working

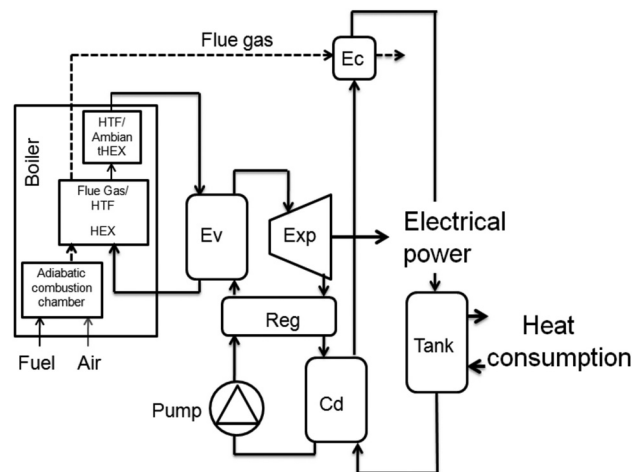


Fig. 4 Configuration of ORC-based CHP

Table 2 Considered fluids and their critical properties

Fluids	T_{crit} (°C)	P_{crit} (kPa)
R236fa	124.9	3198
Isobutane	134.7	3640
n-Butane	152	3796
R245fa	154	3651
HFE7000	164.6	2478
Isopentane	187.2	3370
n-Pentane	196.5	3364
n-Hexane	234.7	3058
n-Heptane	267	2727
OMTS (siloxane fluid)	313.3	1332
Toluene	318.6	4126

fluid. The superheated vapor is expanded into the expander (compressor working in expander mode) and generates electrical energy. A regenerator is used to increase the ORC efficiency [12] and hot water for heating purposes is produced in the condenser and in an additional heat exchanger on the flue gases (economizer). It is supposed that the hot water produced feeds a hot water tank that plays the role of a buffer. This assumption has the corollary that the ORC can always run in nominal regime rather than in part load when the heat demand is lower than the nominal heat capacity of the CHP.

The cycle is, thus, a regenerative, slightly superheated, and sub-cooled Rankine cycle. The following conditions are imposed:

- $\Delta T_{oh} = 5$ K and $\Delta T_{sc} = 5$ K to avoid droplets in the expander and cavitation in the pump
- the efficiency of the regenerator is set to 80%: $\epsilon_{reg} = 0.8$

5 Fluid Selection

The fluid is a critical parameter of an ORC system since it has a strong impact on the design and the performance of the system. Different criteria must be taken into account, such as pressure and density levels, thermodynamic performance, environmental impact, cost, security, etc. [10,12]. The selection of a given working fluid always results in a tradeoff based on selection criteria and on the constraints of the system.

In this study, 11 fluids are considered (see Table 2; the fluid properties are provided by engineering equation solver software). Nonnull ozone depleting potential working fluids have not been considered in this study since they are or will be phased out by the Montreal protocol [10,12].

For the purpose of the working fluid comparison, the following conditions are imposed (T_{cd} is the condensing temperature):

- $T_{cd} = 50$ °C to allow for the production of hot water in the condenser

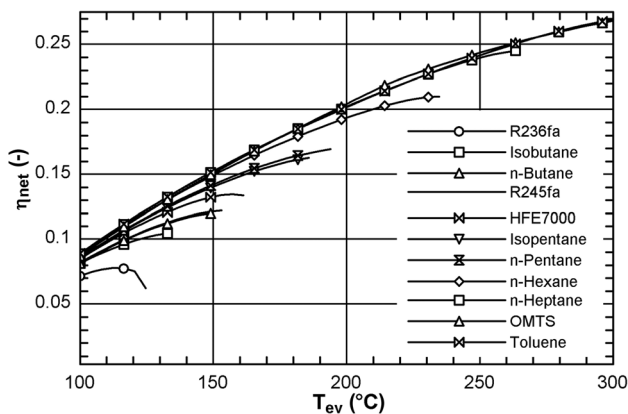


Fig. 5 Evolution of the cycle net efficiency with the evaporating temperature for different fluids ($T_{cd} = 50$ °C)

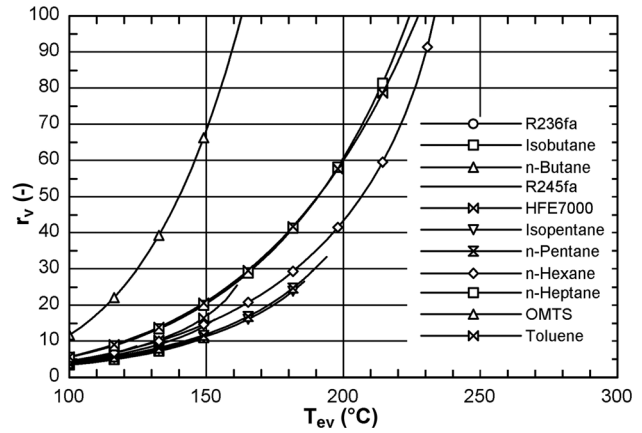


Fig. 6 Volume ratio in term of T_{ev} for different fluids ($T_{cd} = 50$ °C)

- $\epsilon_{s,pp} = 0.7$ and $\epsilon_{s,exp} = 0.7$ to take into account irreversibility of machinery

Figures 5, 6, and 7 show the evolution of three comparison criteria related to the cycle with the evaporating temperature for the considered fluids. These comparison criteria are

- the net cycle efficiency, defined by

$$\eta_{net} = \frac{(w_{exp} - w_{pp})}{q_{ev}} = \frac{(h_{su,exp} - h_{ex,exp}) - (h_{ex,pp} - h_{su,pp})}{h_{su,exp} - h_{ex,pp}} \quad (8)$$

- the volume ratio, as defined above: $r_v = v_{su,exp}/v_{ex,exp}$
- the volume coefficient (Eq. 7)

Table 3 shows that some fluids, such as toluene or n-heptane, show a high efficiency but their volume ratio and volume coefficients are larger. Conversely, fluids such as n-butane or R245fa exhibit a lower efficiency but have volume ratio well suited to scroll expanders and require a lower expander swept volume.

As the considered expander is not a dedicated expander but a compressor adapted into an expander, it is not designed to support high temperatures. This leads to an important limitation; its maximum inlet (in expander mode) temperature is 140 °C. The superheating being set to 5 K this corresponds to a maximum evaporation temperature of 135 °C. This temperature is above the critical point of R236fa and isobutene, which are not considered thereafter (it could be possible to use these fluids in supercritical cycles but this paper focuses only on subcritical cycles). Table 3

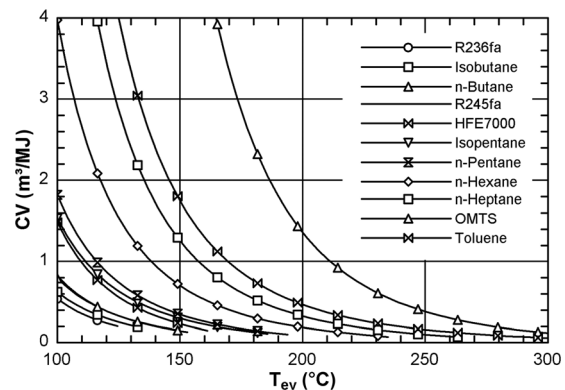


Fig. 7 Evolution of the volume coefficient with the evaporating temperature for different fluids ($T_{cd} = 50$ °C)

Table 3 Characteristics of the basic cycle for different fluids ($T_{cd} = 50^\circ\text{C}$, $T_{ev} = 135^\circ\text{C}$)

Fluid	η_{net} (%)	r_p (-)	r_v (-)	P_{cd} (kPa)	P_{ev} (kPa)	CV_{ORC} (m^3/MJ)
n-Butane	11.36	5.768	7.634	496.6	2865	0.2379
R245fa	11.44	7.482	9.659	343.2	2568	0.2342
HFE7000	12.28	8.537	11.05	166.8	1424	0.3912
Isopentane	12.66	7	8.214	205.2	1436	0.4611
n-Pentane	12.77	7.581	8.585	159.8	1211	0.5383
n-Hexane	13.3	10.1	10.64	53.6	541.4	1.106
n-Heptane	13.51	14.09	14.25	18.9	265.9	2.02
OMTS	13.32	43.39	42.49	0.7	31.5	12.2
Toluene	13.52	15.73	14.71	12.3	194	2.812

shows that the variability of the net efficiency between working fluids is much lower (because this efficiency depends strongly of the temperature levels, which are the same for all the fluids) than that of other parameters such as CV or the volume ratio. Toluene exhibits the highest efficiency but its CV is too high ($CV > 0.82 \text{ m}^3/\text{MJ}$), making it unsuitable to hermetic scroll expanders. In the same manner, octamethylcyclotetrasiloxane (OMTS) is not suited for this application because of its large volume ratio ($r_v > 2.85$) and large volume coefficient (both variables are defined in Sec. 3). The fluid leading for the most compact system is R245fa (it has the lower CV). It also shows a suitable volume ratio and level of pressure.

Values in Table 3 were computed assuming constant expander effectiveness. One method for reducing the number of selection criteria is to consider the real effectiveness curve of the expander since it accounts for the influence of the volume ratio and of the volume coefficient. By using the semiempirical model described in Sec. 2, an ORC using the hermetic expander tested by some of the authors [7] (swept volume: $V_s = 23 \text{ cm}^3$) can be simulated. The results are presented in Table 4. As explained below, when using a scroll expander, there exists an optimal evaporating temperature. It is this temperature that is used if it is below 135°C (see Table 4). Results show that, as expected, fluids with high CV and volume ratio see their cycle efficiency decreased. It appears clear that fluids with a CV higher than $0.89 \text{ m}^3/\text{MJ}$ have a generator efficiency lower than 84%. The value 0 for OMTS is due to the very high CV ($CV = 12.2$, see Table 3) leading to electromechanical and friction losses higher than the shaft power. Finally, the fluid with maximal ORC efficiency is n-pentane, but it gives a less compact system than n-butane or R245fa (the power is lower). From these two last fluids, n-butane shows a slightly better efficiency. However, R245fa is preferred for the present study because of the issues linked to the flammability of n-butane and n-pentane in a domestic micro-CHP unit.

6 Model

This section describes the simulation model of the micro-CHP system.

Table 4 Efficiencies of basic cycle for different fluids with expander model ($T_{cd} = 50^\circ\text{C}$)

Fluid	$\eta_{generator}$ (-)	ϵ_s (%)	η_{net} (%)	\dot{W} (W)	\dot{M} (g/s)	T_{ev} ($^\circ\text{C}$)
n-Butane	87	62.7	9.3	3143	76.7	123
R245fa	87	60.4	8.9	2808	139.6	122
HFE7000	87	54.9	9.2	1958	125.1	131
Isopentane	87	57.4	10.3	2161	50.3	135
n-Pentane	87	56.5	10.3	1827	40.7	135
n-Hexane	78	48.4	9.1	755	19.3	135
n-Heptane	58	33.5	6.4	285	10.3	135
OMTS	0	0	0	0	3.2	135
Toluene	42	24.5	4.7	151	6.7	135

6.1 Boiler. The boiler model [13] associates three subcomponents (Fig. 4):

- one adiabatic combustion chamber
- one flue gases/HTF heat exchanger
- one HTF/ambient heat exchanger (to take into account thermal losses to the environment)

6.1.1 Adiabatic Combustion Chamber. First, the air and the fuel are cooled down or heated up to the reference temperature of 25°C (at which the lower heating value (LHV) is defined) through two fictitious heat exchangers. Corresponding heat fluxes are given by

$$\dot{Q}_1 = \dot{M}_a \cdot c_{p,a} \cdot (T_{ref} - T_{a,su}) \quad (9)$$

$$\dot{Q}_2 = \dot{M}_f \cdot c_{p,f} \cdot (T_{ref} - T_{f,su}) \quad (10)$$

The combustion, supposedly isothermal and complete, releases a heat flux equal to

$$\dot{Q}_3 = -\text{LHV} \cdot \dot{M}_f \quad (11)$$

Finally, flue gases are warmed through a fictive heat exchanger up to the adiabatic flame temperature:

$$\dot{Q}_4 = \dot{M}_g \cdot c_{p,g} \cdot (T_{adiab} - T_{ref}) \quad (12)$$

Where $c_{p,g}$ is the average heat capacity of the flue gases between T_{adiab} and T_{ref} defined by (Eq. (13)) and \dot{M}_g is their mass flow rate, defined by (Eq. (14)).

$$c_{p,g} = \frac{(h_{g,adiab} - h_{g,ref})}{(T_{adiab} - T_{ref})} \quad (13)$$

$$\dot{M}_g = \dot{M}_a + \dot{M}_f \quad (14)$$

Air and flue gases mass flow rates are connected by the fuel air ratio, which can also be expressed in terms of the stoichiometric fuel air ratio and of the excess air:

$$f = \frac{\dot{M}_f}{\dot{M}_a} = \frac{f_{st}}{1 + e} \quad (15)$$

Since the combustion chamber is assumed adiabatic, the sum of each heat flux must be equal to 0:

$$\dot{Q}_1 + \dot{Q}_2 + \dot{Q}_3 + \dot{Q}_4 = 0 \quad (16)$$

6.1.2 Heat Exchanger Gas/HTF. The flue gases leave the combustion chamber to pass through a counterflow heat exchanger that heats up the heat transfer fluid (HTF). This heat exchanger is modeled by means of the ϵ -NTU (number of transfer units) method.

The overall heat transfer coefficient AU is assumed to vary with the mass flow rate of the flue gases, according to the following relation [13]:

$$AU = AU_n \cdot \left(\frac{\dot{M}_g}{\dot{M}_{g,n}} \right)^{0.65} \quad (17)$$

It should be noted that by using this approach, the heat transfer coefficient is a fictive convective heat transfer coefficient that takes into account both convection and radiation.

6.1.3 HTF/Ambient Heat Exchanger. It is assumed that the HTF passes through a second fictitious heat exchanger that represents the ambient losses of the boiler. The heat transfer is modeled

by means of the ϵ -NTU method for semi-isothermal heat exchangers and its overall heat transfer coefficient is assumed to be constant.

6.1.4 Boiler Parameters. The boiler considered in this study is a 22 kW fuel oil boiler tested by the authors.

The fuel oil characteristics are:

- mass concentration: $[C]_m = 86.9\%$; $[H]_m = 13.1\%$
- low heating value: $LHV_f = 42.8 \text{ MJ/kg}$
- specific heat: $cp_f = 1884 \text{ J/(kg}\cdot\text{K)}$

The parameters of the boiler model are identified by minimizing the error on the prediction of the performance of the boiler over a series of 47 tests. For the nominal mass flow rate, the value of one of the 47 test is chosen, this value is $\dot{M}_{g,n} = 0.009885 \text{ kg/s}$.

The identified parameters are:

- nominal heat transfer coefficient of gas/HTF heat exchanger:

$$AU_{og,n} = 34.7 \text{ W/K}$$

- heat transfer coefficient of HTF/ambient heat exchanger:

$$AU_{oa} = 3.3 \text{ W/K}$$

The model with the identified parameters yields very good results with a maximum error of 5 K for exhaust gas temperature and 1 K for exhaust water temperature.

Over the 47 tests, the boiler shows an average efficiency of 92%.

6.2 ORC Heat Exchangers. Heat exchangers of the ORC system are also modeled by the ϵ -NTU method. The evaporator and the condenser are divided into three zones, each zone corresponding to a specific state of the fluid: vapor, two-phase, and liquid [11].

6.3 Expander. In this work, the considered expander is a hermetic scroll machine similar to the one tested and modeled in Sec. 2 and characterized by its effectiveness curves.

6.4 Pump. The pump is assumed to be adiabatic, and its consumption is evaluated by imposing a constant overall isentropic effectiveness (i.e., including electromechanical losses):

$$\dot{W}_{pp} = \frac{\dot{M} \cdot (h_{ex,s} - h_{su})}{\epsilon_{s,pp}} \quad (18)$$

7 Performance Indicators

The first performance indicator is the net efficiency of cycle which is defined by Eq. (8). This efficiency quantifies the performance of the ORC cycle only not the performance of the entire micro-CHP system. Therefore, two other performance indicators are introduced:

Electrical efficiency:

$$\eta_{el} = \frac{\dot{W}_{net}}{\dot{M}_f \cdot LHV_f} \quad (19)$$

Thermal efficiency:

$$\eta_{th} = \frac{\dot{Q}_{heat}}{\dot{M}_f \cdot LHV_f} \quad (20)$$

In the latter formula, \dot{Q}_{heat} is the useful heat power of the CHP system (the total thermal power of the condenser and the economizer available to generate hot water).

The quality of a CHP system is generally evaluated by the primary energy saving (PES) [14]. It represents the economy of primary energy achieved by using CHP in percent of the consumption of the separated production. It is computed by

$$PES = \left(1 - \frac{1}{\frac{\eta_{CHP,th}}{\eta_{ref,th}} + \frac{\eta_{CHP,el}}{\eta_{ref,el}}} \right) \cdot 100 \quad (21)$$

where

- $\eta_{CHP,th}$ is the thermal efficiency of the CHP
- $\eta_{CHP,el}$ is the electrical efficiency of the CHP
- $\eta_{ref,th}$ is the thermal efficiency of a reference separated heat production unit
- $\eta_{ref,el}$ is the electrical efficiency of a reference separated electricity production unit

In the present case, the reference thermal efficiency is the efficiency of the boiler and it is 92%. The reference electrical efficiency is set to 44.2% [14].

8 Optimization

Two main degrees of freedom on the operating conditions are available to optimize the proposed system: the evaporating temperature T_{ev} and the HTF temperature difference between the supply and the exhaust of the evaporator ΔT_{HTF} (or the HTF mass flow rate). The remaining operating conditions are linked to design or technical constraints and do not result from an optimization. Their values are listed in Table 5. For heat exchangers, the effectiveness is set to 0.8 and for the pump, $\epsilon_s = 0.7$.

The influence of T_{ev} on the electrical efficiency is shown in Fig. 8: On the one hand, the ideal cycle efficiency increases with the evaporating temperature, but on the other hand the isentropic effectiveness of the expander exhibits a maximum for a given T_{ev} . Combining these two effects leads to an optimum value for T_{ev} that maximizes the ORC efficiency. In the present case, the optimal evaporating temperature is 122°C.

ΔT_{HTF} also shows an impact on the cycle performance since it impacts the exergy destruction losses due to a poor matching between heating and cooling curves. Figure 9 shows that an optimum value exists, corresponding to HTF temperature profile parallel to the liquid temperature profile of the working fluid. In this case, the value is $\Delta T_{HTF} = 130 \text{ K}$. In future work it would be interesting to optimize this variable to account for HTF pump consumption.

Table 6 summarizes the values of the performance indicators when operating at the optimal performance point ($T_{ev} = 122^\circ\text{C}$ and $\Delta T_{HTF} = 130 \text{ K}$), and with hot water temperatures of 40/30°C in the condenser. This optimal point is chosen as design point and Table 2 also gives the results of the sizing of the main ORC components in terms of expander displacement and heat exchangers heat transfer area. The areas of the different zones of the heat exchangers were computed with typical values (see Table 1) of the transfer coefficients for each zone, as recommended by McMahan [15].

Table 5 Values of inputs parameters for simulations

\dot{M}_f (kg/s)	0.00056
e (–)	0.16
$T_{w,ex}/T_{w,su}$ (°C)	40/30
$\Delta T_{sh}, \Delta T_{sc}$ (K)	5
$\Delta T_{pp,ev}, \Delta T_{pp,cd}$ (K)	10
α_{liquid} (W/m ² /K)	1000
α_{vapor} (W/m ² /K)	140
$\alpha_{two-phase}$ (W/m ² /K)	10,000

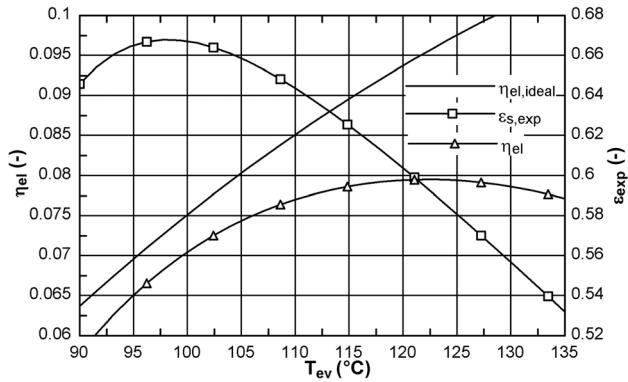


Fig. 8 Influence of T_{ev} on the electrical efficiency

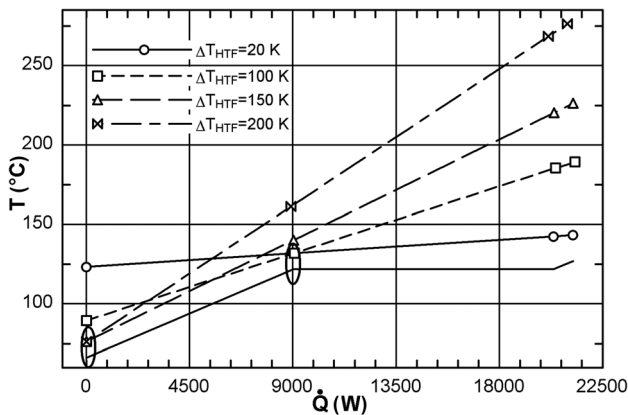


Fig. 9 Temperature profile in the evaporator

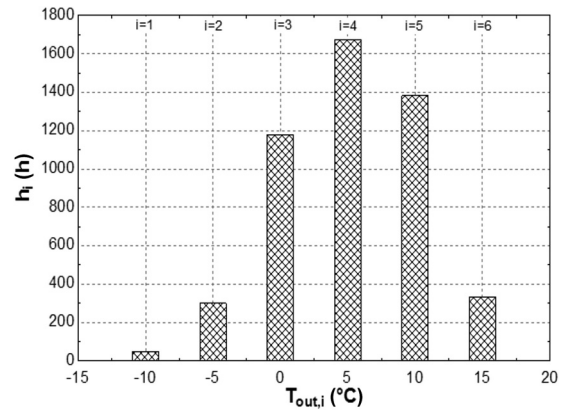


Fig. 10 Average climate (PrEN14825)

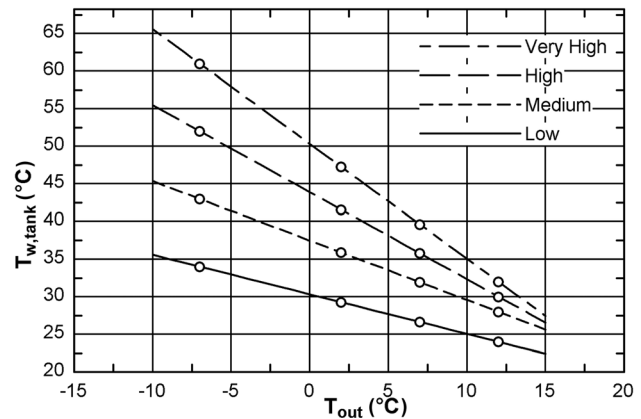


Fig. 11 Heat emitters heating curves

Table 6 Achieved performance and ORC parameters for the design point

Achieved performance		ORC parameters	
η_{ORC} (%)	8.9	V_s (cm ³)	17
η_{el} (%)	7.9	A_{ev} (m ²)	2
η_{th} (%)	87.3	A_{cd} (m ²)	1.8
\dot{W}_{net} (kW)	1.9	A_{reg} (m ²)	2.4

9 Seasonal Simulation

In order to evaluate the seasonal performance of the proposed system, its operation must be simulated over one year. The results of simulation strongly depends on climatic conditions and, thus, on the location and on the control strategy regulating hot water temperatures. The climate can be defined by a “temperature bin” diagram such as the one presented in Fig. 10 for an average European climate as defined by the standard PrEN14825. This diagram indicates the number of hours (bin hours h_i) during which the outdoor temperature is within a range of 5 K (a bin) around the discrete central temperature (the bin temperature $T_{out,i}$). For the purpose of the simulation, four heat emitter heating curves are considered, corresponding to very high, high, medium, and low temperature applications according to the standard PrEN14825 (see Fig. 11). These curves give the hot water temperature leaving the CHP system. This hot water temperature influences the condensing temperature and, thus, the operating condition of the ORC, which affects the efficiency of the system. Finally, a heating demand for each bin ($\dot{Q}_{load,i}$) must be defined. This heating demand depends on the outdoor temperature. Here, a linear profile

is considered: The heat load is 20 kW for an outdoor temperature of -10°C and is null for an outdoor temperature of 20°C .

For each bin, simulation is performed with design point parameters (see Table 2 right column) and it is assumed that the water temperature glide in the system (condenser + economizer) is 10 K. As explained in Sec. 4, it is also assumed that, through the use of a buffer tank, the CHP system always operates at full load.

Figure 12 shows the evolution of the electrical efficiency in terms of outdoor temperature for each bin. The electrical efficiency of the system varies from 6.35% for a hot water temperature of 65°C ($T_{out} = -10^\circ\text{C}$, bin 1, very high temperature application) to 8.6% for a hot water temperature of 22°C ($T_{out} = -15^\circ\text{C}$, bin 6, low temperature application). Corresponding net electrical powers vary from 1.5 kW to 2.05 kW.

The overall efficiencies, which are the efficiencies of the micro-CHP system during one year, are computed as follows:

$$\eta_{el,overall} = \frac{\sum_{i=1}^n (\text{RunTime}_i \cdot \dot{W}_{net,i})}{\left(\sum_{i=1}^n \text{RunTime}_i \right) \cdot \text{LHV}_f \cdot \dot{M}_f} \quad (22)$$

$$\eta_{th,overall} = \frac{\sum_{i=1}^n (\text{RunTime}_i \cdot \dot{Q}_{heat,i})}{\left(\sum_{i=1}^n \text{RunTime}_i \right) \cdot \text{LHV}_f \cdot \dot{M}_f} \quad (23)$$

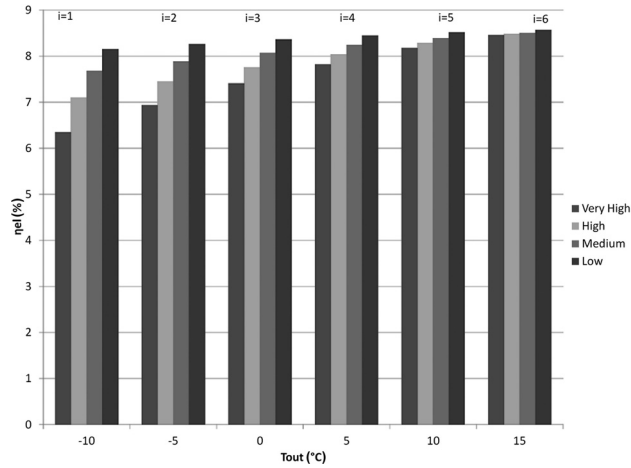


Fig. 12 Electrical efficiency for each bin in term of outdoor temperature for four heat emitter heating curves (very high, high, medium, and low temperature application)

Table 7 Results of seasonal simulation

Application	$\eta_{el,overall}$ (%)	$\eta_{th,overall}$ (%)	PES
Low temperature	8.4	87.3	12.2
Medium temperature	8.16	87.26	11.75
High temperature	7.92	87.27	11.33
Very high temperature	7.64	87.3	10.85

where n is the amount of bin; here $n = 6$, and RunTime is the necessary time to fulfill the heat demand computed as RunTime; $= \dot{Q}_{load,i} \cdot h_i / \dot{Q}_{heat,i}$.

The results for seasonal simulation are summarized in Table 7. The electrical efficiency is about 8% and the variation in electrical efficiency between low and very high temperature applications is 0.8 point. The system allows saving about 11% of primary energy compared to a separate production. The electrical efficiency is relatively low compared to ICE (about 30%) and needs to be improved to allow ORC-based CHP be profitable. However, this low efficiency could in some cases be counterbalanced by the fact that solid fuels can be used in an ORC and not in an ICE.

10 Improvement Potential

The considered expander is a compressor adapted into an expander, not a dedicated expander designed for ORC working conditions. As a consequence, it is not optimized for expander applications. The goal of this section is to quantify the performance increase of the system for different improvements on the scroll machine.

10.1 Increase of the Maximum Inlet Temperature. The maximum temperature of currently available hermetic scroll machines (compressor outlet or expander inlet) is 140°C. Therefore, all the previous simulations were performed with expander inlet temperatures inferior or equal to this temperature, which constitutes an important limitation for the cycle. Fig. 5 shows that the net ORC cycle efficiency computed with $\epsilon_{s,exp} = 0.7$ increases with the evaporating temperature. A higher maximum allowed temperature would, therefore, be profitable to cycle performance.

However, Fig. 13 shows that the efficiency, computed with the actual expander isentropic effectiveness (computed with the expander model), increases but remains limited, and for all the fluids an optimum exists after which the net efficiency decreases. This is due to the effect of underexpansion losses at high pressure ratios: As shown in Fig. 14, the expander isentropic effectiveness

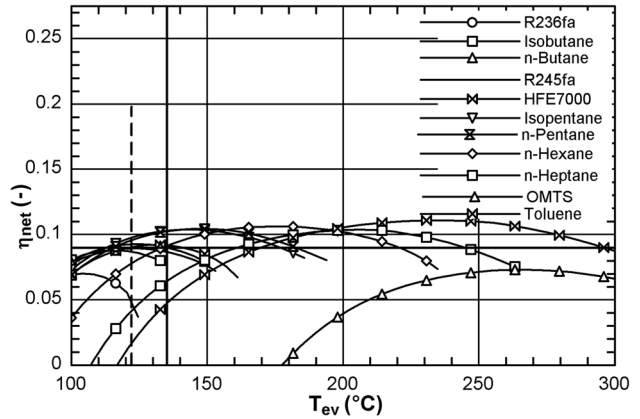


Fig. 13 Net ORC efficiency versus T_{ev} with actual scroll expander ($T_{cd} = 50^\circ\text{C}$)

decreases sharply when the expander is operated at high evaporating temperatures. Moreover, fluids with high CV (see Fig. 7) give a null net efficiency at low temperatures. This statement is due to unsuitable CV and r_v of the expander for the considered operating conditions.

10.2 Use Two Expanders in Series. Using two expanders in series can lead to better efficiencies: For working fluids presenting a high volume ratio, assembling two expanders in series is equivalent to increasing the internal volume ratio and, thus, decreasing the under expansion losses. Figure 15 shows the evolution of the overall isentropic effectiveness (isentropic effectiveness over the two expanders in series) in terms of evaporating temperature for toluene and n-pentane. This curve shows that using two expanders leads to a better isentropic effectiveness but only for high temperature. Indeed, for low temperature, the efficiency is lower compared to the efficiency with one expander.

This increase of isentropic effectiveness gives higher net efficiency of the ORC (see Fig. 16): The net efficiency is about 10% at 180°C for n-pentane and reaches about 13% for toluene at 270°C. For the studied working conditions, using two expanders in series is, thus, interesting if the maximal inlet temperature of the expander is higher than 135°C.

10.3 Adaptation of CV. Generally speaking, the higher the critical temperature, the lower the fluid density at a given temperature and, thus, the lower the volume coefficient (CV_{ORC}). It might be interesting to adapt the CV of the expander to these fluids in order to increase the performance. Adapting the CV of the

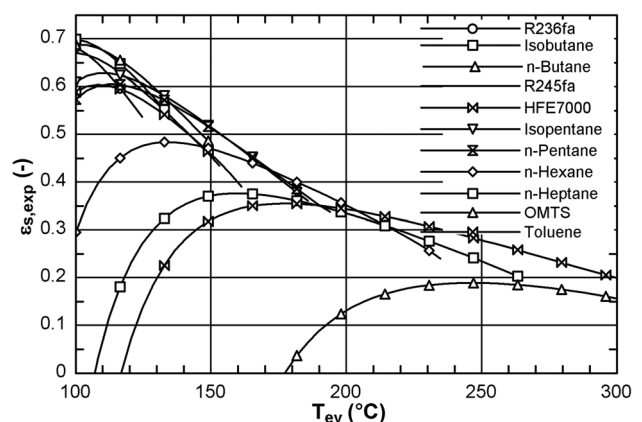


Fig. 14 Isentropic effectiveness of the actual scroll expander in terms of T_{ev} for different fluid ($T_{cd} = 50^\circ\text{C}$)

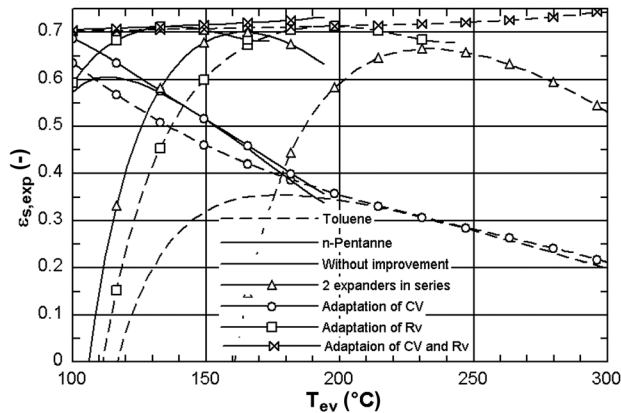


Fig. 15 Improvement of the isentropic effectiveness for toluene and n-pentane ($T_{cd} = 50^\circ\text{C}$)

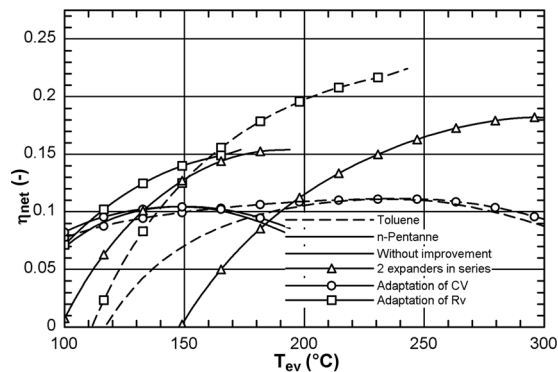


Fig. 16 ORC net efficiency with improvement for toluene and n-pentane ($T_{cd} = 50^\circ\text{C}$)

expander actually means adapting the power of the electric motor of the hermetic engine. Indeed, the asynchronous motor is sized only for three different fluids with comparable density in compressor mode and is undersized in expander mode [16]. By imposing the generator efficiency at its maximum value ($\eta_{generator} = 87.3\%$) in the semiempirical model described in Sec. 2, the isentropic effectiveness computed with an adapted CV is found. This is done for toluene and n-pentane and the results are presented in Fig. 15. It appears that the effectiveness at low temperature, where the CV_{ORC} is high, has increased. The optimum temperatures for both fluids are all similar. This optimum temperature is in fact the temperature that gives a volume ratio well suited to expander volume ratio. The ORC net efficiencies computed with adapted CV are shown in Fig. 16.

10.4 Adaptation of $r_{v,in}$. The external volume ratios achieved by considered fluids at $T_{ev} = 135^\circ\text{C}$ are slightly higher than the optimal ones but they are relatively well adapted to the studied expander. However, if the evaporating temperature increases, this external volume ratio increases and the isentropic effectiveness decreases (Fig. 14 and Fig. 15). By imposing the built-in volume ratio of the expander equal to the external volume ratio in the semiempirical model of Sec. 2, the isentropic effectiveness with adapted $r_{v,in}$ is found. Figure 15 shows this expander isentropic effectiveness that is null at low temperatures for fluid with a high CV but reaches more than 70% at higher temperatures. In this case, the optimal temperature is the one that gives the best CV, thus, the best electromechanical efficiency. Figure 16 shows the net efficiency computed with an adapted internal built-in volume ratio. It shows that the potential of improvement is significant for both fluids. A net efficiency of 10% can be reached if the

evaporating temperature is increased up to 170°C . For this temperature, the internal volume ratio must be close to 10.

10.5 Adaptation of CV and Rv. If CV_{exp} and $r_{v,in}$ of the expander are both adapted to the external conditions, the isentropic efficiencies achieved with both fluids is close to 70% on the whole temperature range (see Fig. 15), and thus, the calculation of net efficiency gives similar results to those indicated in Fig. 5.

10.6 Seasonal Simulation for Two Expanders in Series. In Sec. 10.2, the interest of using two expanders in series was highlighted. To evaluate the benefits of such a configuration, a seasonal simulation is performed with n-pentane, an evaporating temperature of 195°C , and a medium temperature application. The overall efficiencies are $\eta_{ei,g} = 12.5\%$ and $\eta_{th,g} = 79\%$ and the PES = 12.4%. This represents a 58% increase of the electrical efficiency. This example shows the interest to develop purpose designed expanders to increase the performance of combined heat and power ORCs.

11 Conclusion

ORC is a technology well suited to micro-CHP in competition with Stirling technologies. ORC-based CHP systems are under development by several manufacturers announcing mass commercialization in the coming years. The goal of this paper was to evaluate the pertinence of using hermetic, lubricated scroll expanders for such systems since they are particularly well adapted to domestic micro-scale Rankine cycle applications (electrical powers lower than 50 kW) in terms of capacity and displacement.

A model of an ORC-based micro-CHP unit was developed by associating a validated model of an ORC system and a fuel oil boiler. This model was used to optimize and size the system and to perform seasonal simulations. These seasonal simulations were performed for an average European climate and four heat emitter heating curves according to the standard PrEN14825. The results show that the electrical efficiency of the system varies from 6.35% when producing hot water at 65°C to 8.6% when producing a hot water at a temperature of 22°C . The system shows an overall electrical efficiency of about 8% and a thermal efficiency of about 87% without significant difference between the four heat emitter heating curves. The micro-CHP system allows saving 11.8% of primary energy compared to a separate production.

Improvements of the expander were then proposed to evaluate the performance of a purpose designed machine instead of a compressor running in reverse. The first improvement is the rise of maximum inlet temperature of the scroll, which would allow raising the evaporating temperature. Indeed, this temperature is limited to 140°C , which limits the evaporation pressure. In particular, increasing this temperature allows using two scroll expanders in series. Seasonal simulation with two-stage expansion, n-pentane, and a maximum temperature of 195°C led to an electrical efficiency of 12.5% compared to 7.9% in the single-stage configuration. Others required improvement are the adaptation of CV, in other words, the proper sizing of the asynchronous machine of the hermetic engine to avoid too large electromechanical losses. A last improvement is the rise of the built-in volume ratio to avoid under expansion losses.

This study showed that hermetic scroll expanders are well suited for small ORC systems with evaporating temperature about 130°C . However, for an ORC-based micro-CHP system, the evaporating temperature must be above 130°C to achieve good electrical efficiency. Purpose-designed hermetic scroll expanders should, therefore, be developed in order to increase their maximum inlet temperature, their built-in volume ratio, and to maximize the cycle efficiency.

Nomenclature

- A = area (m^2)
- AU = heat transfer coefficient (W/K)

CV = volume coefficient (m^3/J)
 cp = specific heat ($\text{J}/\text{kg}/\text{K}$)
 e = air excess
 FF = filling factor
 f = fuel air ratio
 h = specific enthalpy (J/kg)
 LHV = low heating value (J/kg)
 \dot{M} = mass flow rate (kg)
 ODP = ozone depletion potential
 P = pressure (Pa)
 PES = primary energy saving (%)
 \dot{Q} = heat flux (W)
 q = heat (J)
 r = ratio
 T = temperature ($^{\circ}\text{C}$)
 V = volume (m^3)
 v = specific volume (m^3/kg)
 \dot{V} = volume flow rate (m^3/s)
 \dot{W} = mechanical power (W)
 w = specific work (J/kg)

Greek Letters

α = convective heat transfer coefficient ($\text{W}/(\text{m}^2\cdot\text{K})$)
 Δ = difference
 ϵ = effectiveness
 η = efficiency

Subscripts

a = air
 adiab = adiabatic
 Amb = Ambient
 CHP = combined heat and power
 cd = condenser
 crit = critical
 el = electric
 ev = evaporator
 ex = exhaust
 exp = expander
 f = fuel
 g = flue gases
 heat = heating
 in = internal
 n = nominal
 oh = over heating
 p = pressure
 pp = pump or pinch point
 ref = reference
 reg = regenerator
 s = isentropic or swept
 sc = subcooling
 sh = shaft
 st = stoichiometric

su = supply
 th = thermal
 v = volume
 w = water

Acronyms

HTF = heat transfer fluid
 ORC = organic Rankine cycle
 CHP = combined heat and power

References

- [1] De Paepe, M., and Mertens, D., 2007, "Combined Heat and Power in a Liberalized Energy Market," *J. Energy Convers. Manage.*, **48**, pp. 2542–2555.
- [2] Siemers, W., 2007, "Technical and Economic Comparison of Different Technologies for Micro-CHP," internal research paper, CUTEC-Institut, Clausthal-Zellerfeld, Germany.
- [3] Liu, H., Qiu, G., Shao, Y., Daminabo, F., and Riffat, S. B., 2010, "Preliminary Experimental Investigations of a Biogas-Fired Micro-Scale CHP With Organic Rankine Cycle," *Int. J. Low-Carb. Tech.*, **5**, pp. 81–87.
- [4] Lombardi, K., Ugursal, V. I., and Beausoleil-Morrison, I., 2008, "Performance and Emissions Testing of 1 kWe Stirling Engine," Proc. Micro-Cogeneration, Ottawa, Canada, April 29–May 1.
- [5] Andlauer, B., Stabat, P., Marchio, D., and Flament, B., 2010, "Multi-Objective Optimization Procedures for Sizing Operating Building-Integrated Micro-Cogeneration Systems," Proc. 8th International Conference on System in Buildings, Liège, Belgium, December 13–15.
- [6] Simader, G., Krawinkler, R., and Trnka, G., 2006, "Micro CHP Systems: State-of-the-Art," Deliverable 8 (D8) of Green Lodges Project (EIE/04/252/S07.38608), Austrian Energy Agency, Vienna, Austria, March.
- [7] Lemort, V., Quoïlin, S., and Declaye, S., 2012, "Experimental Characterization of a Hermetic Scroll Expander for Use in a Micro-Scale Rankine Cycle," *J. Power Energ.*, **226**, pp. 126–136.
- [8] Lemort, V., Quoïlin, S., Cuevas, C., and Lebrun, J., 2009, "Testing and Modeling of a Scroll Expander Integrated Into an Organic Rankine Cycle," *J. Appl. Therm. Eng.*, **29**, pp. 3094–3102.
- [9] Zanelli, R., and Favrat, D., 1994, "Experimental Investigation of a Hermetic Scroll Expander-Generator," 12th International Compressor Engineering Conference, Purdue University, West Lafayette, IN, July 12–19, pp. 459–464.
- [10] Quoïlin, S., Declaye, S., and Lemort, V., 2010, "Expansion Machine and Fluid Selection for the Organic Rankine Cycle," Proc. 7th International Conference on Heat Transfer, Fluid Mechanics and Thermodynamics, Antalya, Turkey, July 19–21.
- [11] Quoïlin, S., Lemort, V., and Lebrun, J., 2010, "Experimental Study and Modeling of an Organic Rankine Cycle Using Scroll Expander," *J. Appl. Energ.*, **87**, pp. 1260–1268.
- [12] Aoun, B., 2008, "Micro Cogénération pour les batiments résidentiels fonctionnant avec des energie renouvelables," Ph.D. thesis, Ecole des Mines de Paris, Paris.
- [13] Lebrun, J., Bourdouxhe, J. P., and Grodent, M., 1999, "HVAC1KIT—A Toolkit for Primary HVAC System Energy Calculation," prepared for ASHRAE TC 4.7 Energy Calculation, Laboratory of Thermodynamics, University of Liège, Liège, Belgium.
- [14] European Parliament and Council, 2007, "Commission Decision of 21 December 2006 Establishing Harmonised Efficiency Reference Values for Separate Production of Electricity and Heat in Application of Directive 2004/8/EC of the European Parliament and of the Council," Document number C(2006) 6817), OJ L **32**, 6.2.2007, pp. 183–188.
- [15] McMahan, A., 2006, "Design & Optimization of Organic Rankine Cycle Solar-Thermal Powerplants," Ph.D. thesis, University of Wisconsin-Madison, Madison, WI.
- [16] Quoïlin, S., 2011, "Sustainable Energy Conversion Through the Use of Organic Ranking Cycles for Waste Heat Recovery and Sola Applications," Ph.D. thesis, University of Liège, Liège, Belgium.